Supporting Information

Zha et al. 10.1073/pnas.1019293108

A.

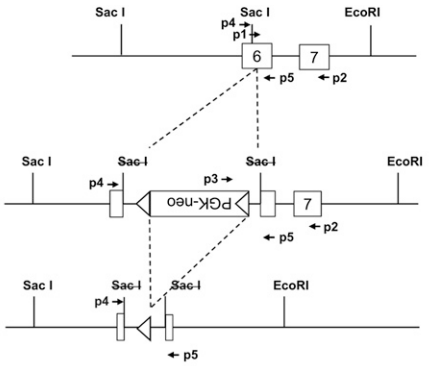

B.

	5' to 3' Sequence	Products
P1	GAAAAAGTCTATGAGCTCCTGGGAG	P1+P2=261bp in WT and no product in either Δneo or knockout allele. P3+P2~370bp in original knockout allele. The SacI site is underlined.
P2	CCCTTCAGACAGCCAGCTAAGACAG	
P3	ACGTAAACTCCTCTTCAGACCT	
P4	CATGGAGGTTCAGGGACTCA	P4+P5=281bp in WT and ~420bp in Δneo and no product in original knockout allele
P5	GTTCTCCCAGAAAAGCTCGG	
NeoF	AAGATGGATTGCACGCAGGTT	NeoF+NeoR= 623bp within the neo resistant gene
NeoR	CCGGCCACAGTCGATGAAT	

C.

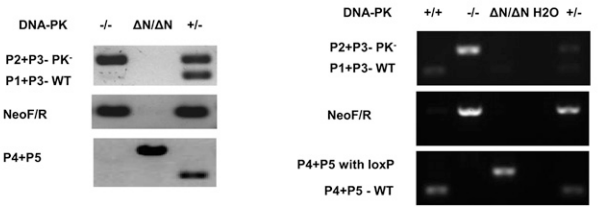

Fig. S1. (Continued)

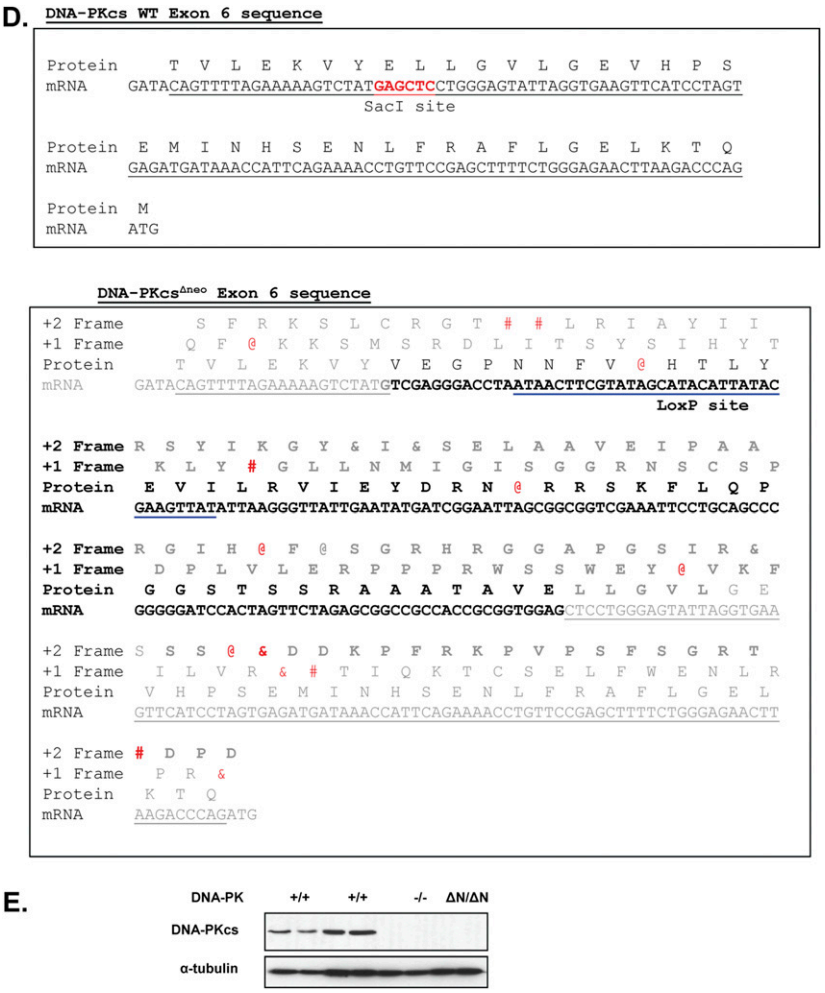

Fig. S1. Analyses of the DNA-PK catalytic subunit$^{\Delta Neo}$ (PKcs) allele. (*A*) Schematic presentation of the WT DNA-PKcs locus, initial DNA-PKcs–targeted allele, and deleted-neo allele. Exon 6 and exon 7 of murine DNA-PKcs, the SacI site at which the loxp-pGK-neo-loxp was introduced, and all of the primers used in the analyses were diagrammed. (*B*) The list of primers used in the analyses. The SacI site within P1 at exon 6 of the WT DNA-PKcs allele is underlined. NeoF and NeoR are both located within the phosphoglycerate kinase (pGK)-Neo cassette. (*C*) The results of two representative PCR analyses of WT, DNA-PK$^{-/-}$, and DNA-PKcs$^{\Delta neo/\Delta neo}$ cells. (*D*) The sequence of the WT (*Upper*) and DNA-PKcs$^{\Delta neo}$ (*Lower*) allele at the exon 6 region. The back/gray underline indicates the original exon 6 sequence. The black and bold area in *Lower* represents the sequence inserted into exon 6 of the DNA-PKcs$^{\Delta neo}$ allele. The blue underline indicates the residual loxP site after Cre recombination. The SacI site is marked in red in the WT sequence. The protein sequence encoded by this region is marked above the mRNA sequence (as protein). In the case of the DNA-PKcs$^{\Delta neo}$ allele, the two other possible translational frames (+1 and +2 frame) are also marked. Translational termination signals (@, TAG; #, TAA; &, TGA) are in red in *Lower*.(*E*) Western blot for total DNA-PKcs protein in DNA-PK$^{+/+,\ -/-}$, or $^{\Delta neo/\Delta neo}$ ES cells. Antibodies are from EMD (anti-alpha-tubulin) and Thermo Scientific (Ab-4, anti-DNA-PKcs).

JH290 Coding Join Substrate		Amp^r	Cam^r&Amp^r	Cam/Amp	Relative Level
Exp1	WT(TC1)	39400	450	1.14%	
	DNA-PK$^{-/-}$	22100	10	0.05%	0.04
	DNA-PK$^{\Delta N/\Delta N}$	28500	7	0.02%	0.02
	XRCC4-/-	6500	1	0.02%	0.01
Exp2	WT(TC1)	5500	39	0.71%	
	DNA-PK$^{-/-}$	4800	2	0.04%	0.06
	DNA-PK$^{\Delta N/\Delta N}$	6800	2	0.03%	0.04
	DNA-PK$^{\Delta N/\Delta N}$(no Rag)	7100	0	0.00%	<0.002
Exp3	WT(TC1)	12300	124	1.01%	
	DNA-PK$^{-/-}$	9800	6	0.06%	0.06
	DNA-PK$^{\Delta N/\Delta N}$	5600	4	0.07%	0.07
	XRCC4$^{-/-}$	2800	0	0.00%	<0.010

Fig. S2. DNA-PKcs$^{\Delta neo/\Delta neo}$ ES cells are impaired for extrachromosomal coding join formation. The results of extrachromosomal variable (diversity) joining [V(D)J] recombination analyses using coding join substrate (JH290) in WT, DNA-PK$^{-/-}$, DNA-PKcs$^{\Delta neo/\Delta neo}$, and control XRCC4$^{-/-}$ ES cells.

		ATMi	Amp^r	Cam^r&Amp^r	Cam/Amp	Relative Level
Exp1	WT(TC1)	-	45000	563	1.25%	
	DNA-PK$^{\Delta N/\Delta N}$	-	14000	173	1.24%	0.99
	DNA-PK$^{\Delta N/\Delta N}$	+	131000	126	0.10%	0.08
	DNA-PK$^{\Delta N/\Delta N}$ (no Rag)	-	66000	0	0.00%	<0.001
	XRCC4-/-	-	6500	1	0.02%	0.01
Exp2	WT(TC1)	-	123000	725	0.59%	
	WT(TC1)	+	50000	622	1.24%	2.11
	DNA-PK$^{\Delta N/\Delta N}$		69000	331	0.48%	0.82
	DNA-PK$^{\Delta N/\Delta N}$	+	124000	103	0.08%	0.14
	DNA-PK$^{\Delta N/\Delta N}$ ATM$^{-/-}$	-	69000	47	0.07%	0.12
	DNA-PK$^{\Delta N/\Delta N}$ (no Rag)	-	121000	0	0.00%	<0.014
Exp3	WT(TC1)	-	21000	258	1.23%	
	WT(TC1)	+	25000	485	1.94%	1.58
	DNA-PK$^{\Delta N/\Delta N}$		17000	47	0.28%	0.23
	DNA-PK$^{\Delta N/\Delta N}$	+	11000	10	0.09%	0.07
	DNA-PK$^{\Delta N/\Delta N}$ ATM$^{-/-}$	-	9000	3	0.03%	0.03
	DNA-PK$^{\Delta N/\Delta N}$ (no Rag)	-	7000	1	0.01%	<0.011
Exp 4	WT(TC1)	-	3700	40	1.08%	
	ATM$^{-/-}$	-	6400	68	1.06%	0.98
	DNA-PK$^{\Delta N/\Delta N}$	-	4900	28	0.57%	0.53
	DNA-PK$^{\Delta N/\Delta N}$ ATM$^{-/-}$	-	3800	4	0.11%	0.10
	XRCC4$^{-/-}$	-	3900	0	0.00%	<0.024
Exp 5	WT(TC1)	-	2400	20	0.83%	
	ATM$^{-/-}$	-	2200	19	0.86%	1.04
	DNA-PK$^{\Delta N/\Delta N}$	-	2800	27	0.96%	1.16
	DNA-PK$^{\Delta N/\Delta N}$ ATM$^{-/-}$	-	4400	4	0.09%	0.11
	XRCC4$^{-/-}$	-	2900	1	0.03%	0.04
Exp 6	WT(TC1)	-	2400	44	1.83%	
	WT(TC1)	+	2100	35	1.67%	0.91
	ATM$^{-/-}$	-	3300	46	1.39%	0.76
	DNA-PK$^{\Delta N/\Delta N}$	-	4500	64	1.42%	0.78
	DNA-PK$^{\Delta N/\Delta N}$	+	2600	6	0.23%	0.13
	XRCC4$^{-/-}$	-	3900	1	0.03%	0.01

Fig. S3. Ataxia telangiectasia-mutated (ATM) kinase promotes efficient extrachromosomal SJ formation in DNA-PKcs–deficient ES cells. The result of extrachromosomal V(D)J analyses with a signal join substrate (JH200) in WT, ATM$^{-/-}$, DNA-PKcs$^{\Delta neo/\Delta neo}$ (with or without ATM inhibitor), DNA-PKcs$^{\Delta neo/\Delta neo}$ATM$^{-/-}$, and control XRCC4$^{-/-}$ ES cells.

Genotypes	Left RSignaling Flank	Right Signaling Flank	#	Del bp
Precise Junction	TGTTTTTGTTCCAGTCTGTAGCACTGTG	CACAGTGGTAGTACTCCACTGTCTGGCTGTACAAAAACC		
DNA-PK$^{\Delta N/\Delta N}$	TGTTTTTGTTCCAGTCTGTAGCACTGTG	CACAGTGGTAGTACTCCACTGTCTGGCTGTACAAAAACC	13	0
	TGTTTTTGTTCCAGTCTGTAGCACTGT	CACAGTGGTAGTACTCCACTGTCTGGCTGTACAAAAACC	1	1
DNA-PK$^{\Delta N/\Delta N}$, ATMi	TGTTTTTGTTCCAGTCTGTAGCACTGTG	CACAGTGGTAGTACTCCACTGTCTGGCTGTACAAAAACC	8	0
	TGTTTTTGTTCCAGTCTGTAGCAC	CACAGTGGTAGTACTCCACTGTCTGGCTGTACAAAAACC	1	4
	TGTTTTTGTTCCAGTCT	AGTGGTAGTACTCCACTGTCTGGCTGTACAAAAACC	2	14
	TGTTTTTGTTCCAGT	GTAGTACTCCACTGTCTGGCTGTACAAAAACC	1	20
DNA-PK$^{\Delta N/\Delta N}$ATM$^{-/-}$	TGTTTTTGTTCCAGTCTGTAGCACTGTG	CACAGTGGTAGTACTCCACTGTCTGGCTGTACAAAAACC	9	0
	TGTTTTTGTTCCAGTCTGTAGCACTGTG	AGTGGTAGTACTCCACTGTCTGGCTGTACAAAAACC	1	3
	TGTTTTTGTTCCAGTCTGTAGCACTG	CACAGTGGTAGTACTCCACTGTCTGGCTGTACAAAAACC	1	2
	TGTTTTTGTTCCAGTCTGTAGCACT	ACAGTGGTAGTACTCCACTGTCTGGCTGTACAAAAACC	2	4
	TGTTTTTGTTCCAGTCTGTAGCA	AGTGGTAGTACTCCACTGTCTGGCTGTACAAAAACC	1	8
	TGTTTTTGTTCCAGTCTGTAGC	GTACTCCACTGTCTGGCTGTACAAAAACC	1	16
	TGTTTTTGTTCCAGTCTGTAG	ACTCCACTGTCTGGCTGTACAAAAACC	1	19
	TGTTTTTGTTCCAGTC	GTACAAAAACC	1	41
	TGTTTTT	AAAACC	1	55

Fig. S4. Sequence analysis of extrachromosomal V(D)J signal joints from DNA-PKcs$^{\Delta neo/\Delta neo}$ (with or without ATM inhibitor) and DNA-PKcs$^{\Delta neo/\Delta neo}$ATM$^{-/-}$ ES cells. The number of base pairs deleted at each junction is marked on the right most column. The number in the # column indicates the number of clones sequenced that represented the given sequence.

Genotypes	#	Left	N	Right	Del.bp
GL		GGTTTTTGTTCCAGTCTGTAGCACTGTG		CACAGTGGTAGTACTCCACTGTCTGGCTGTACAAAAACC	
DNA-PK$^{-/-}$	28	GGTTTTTGTTCCAGTCTGTAGCACTGTG		CACAGTGGTAGTACTCCACTGTCTGGCTGTACAAAAACC	0
ATM$^{C/C}$	1	GGTTTTTGTTCCAGTCTGTAGCACTGTG	G	CACAGTGGTAGTACTCCACTGTCTGGCTGTACAAAAACC	0
	1	GGTTTTTGTTCCAGTCTGTAGCACTGTG	A	CACAGTGGTAGTACTCCACTGTCTGGCTGTACAAAAACC	0
	1	GGTTTTTGTTCCAGTCTGTAGCACTGTG	CG	CACAGTGGTAGTACTCCACTGTCTGGCTGTACAAAAACC	0
	1	GGTTTTTGTTCCAGTCTGTAGCACTGTG	GG	CACAGTGGTAGTACTCCACTGTCTGGCTGTACAAAAACC	0
	1	GGTTTTTGTTCCAGTCTGTAGCACTGTG	GC	CACAGTGGTAGTACTCCACTGTCTGGCTGTACAAAAACC	0
	1	GGTTTTTGTTCCAGTCTGTAGCACTGTG	AC	CACAGTGGTAGTACTCCACTGTCTGGCTGTACAAAAACC	0
	1	GGTTTTTGTTCCAGTCTGTAGCACTGTG		ACAGTGGTAGTACTCCACTGTCTGGCTGTACAAAAACC	1
	1	GGTTTTTGTTCCAGTCTGTAGCACTGT	G	CAGTGGTAGTACTCCACTGTCTGGCTGTACAAAAACC	2
DNA-PK$^{-/-}$	29	GGTTTTTGTTCCAGTCTGTAGCACTGTG		CACAGTGGTAGTACTCCACTGTCTGGCTGTACAAAAACC	0
ATM$^{-/-}$	1	GGTTTTTGTTCCAGTCTGTAGCACTGTG	TT	CACAGTGGTAGTACTCCACTGTCTGGCTGTACAAAAACC	0
	1	GGTTTTTGTTCCAGTCTGTAGCACTGTG	TA	CACAGTGGTAGTACTCCACTGTCTGGCTGTACAAAAACC	0
	1	GGTTTTTGTTCCAGTCTGTAGCACTGTG	G	CACAGTGGTAGTACTCCACTGTCTGGCTGTACAAAAACC	0
	1	GGTTTTTGTTCCAGTCTGTAGCACTGT	A	ACAGTGGTAGTACTCCACTGTCTGGCTGTACAAAAACC	2
	2	GGTTTTTGTTCCAGTCTGTAGCACTGT	T	CAGTGGTAGTACTCCACTGTCTGGCTGTACAAAAACC	3
	1	GGTTTTTGTTCCAGTCTGTAGCACTG		CAGTGGTAGTACTCCACTGTCTGGCTGTACAAAAACC	4
	1	GGTTTTTGTTCCAGTCTGTAG	A	ACAGTGGTAGTACTCCACTGTCTGGCTGTACAAAAACC	8
	1	GGTTTTTGTTCCAGTCTGTAGCACTGT	C	AGTACTCCACTGTCTGGCTGTACAAAAACC	9
	1	GGTTTTTGTTCCAGTCTGTAGC	C	GTGGTAGTACTCCACTGTCTGGCTGTACAAAAACC	10
	1	GGTTTTTGTTCCAGTCTG		CCACTGTCTGGCTGTACAAAAACC	24

Fig. S5. Sequence analysis of chromosomal V(D)J signal joints from DNA-PKcs$^{-/-}$ATM$^{C/C}$ and DNA-PKcs$^{-/-}$ATM$^{-/-}$ v-abl transformed pro-B cells. The number of base pairs deleted at the junctions is marked in the Del bp column. The number in the # column indicates the number of clones sequenced that represented the given sequence.

Genotypes		Left	N	Right	Del.bp
GL	#	GGTTTTTGTTCCAGTCTGTAGCACTGTG		CACAGTGGTAGTACTCCACTGTCTGGCTGTACAAAAACC	
ATM$^{-/-}$	15	GGTTTTTGTTCCAGTCTGTAGCACTGTG		CACAGTGGTAGTACTCCACTGTCTGGCTGTACAAAAACC	0
	1	GGTTTTTGTTCCAGTCTGTAGCACTGTG	C	CACAGTGGTAGTACTCCACTGTCTGGCTGTACAAAAACC	0
ATM$^{-/-}$:NU7441	8	GGTTTTTGTTCCAGTCTGTAGCACTGTG		CACAGTGGTAGTACTCCACTGTCTGGCTGTACAAAAACC	0
	1	GGTTTTTGTTCCAGTCTGTAGCACTGT	T	ACAGTGGTAGTACTCCACTGTCTGGCTGTACAAAAACC	2
	1	GGTTTTTGTTCCAGTCTGTAGCACTGT		CAGTGGTAGTACTCCACTGTCTGGCTGTACAAAAACC	3
	1	GGTTTTTGTTCCAGTCTGTAGCAC	C	AGTGGTAGTACTCCACTGTCTGGCTGTACAAAAACC	7
	1	GGTTTTTGTTCCAGTCTGTA		AGTACTCCACTGTCTGGCTGTACAAAAACC	17

Fig. S6. Sequence analysis of chromosomal V(D)J signal joints from ATM$^{-/-}$ v-abl transformed pro-B cells with or without DNA-PKcs inhibitor NU7441. The number of base pairs deleted at the junction is marked on the Del bp column. The number in the # column indicates the number of clones sequenced that represented the given sequence.

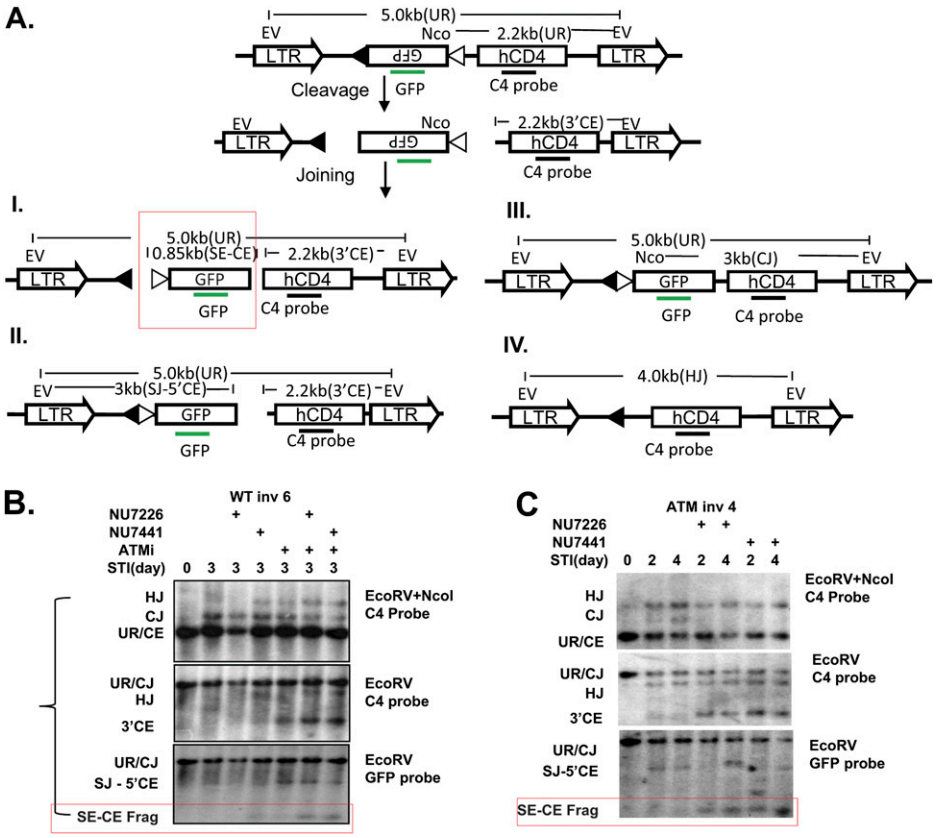

Fig. S7. DNA-PK kinase inhibitor reduced SJ formation during inversional V(D)J recombination in v-abl–transformed pro-B lines. (*A*) Diagram of the pMX-INV substrate used in chromosomal V(D)J recombination assays. The diagram is adapted from Bredemeyer et al. (1). The pMX-INV vector has a single pair of recombination signal sequences (RSs) flanking the inverted GFP cassette. The long terminal repeats (LTR), IRES-hCD4 cDNA (hCD4), 5′ 12-recombination signal (12-RS), and 3′ 23-RS (filled and open triangles, respectively), EcoRV (EV) site, NcoI (Nco) site, and C4 and GFP probes are indicated. Normal V(D)J recombination between the two RSs and successful formation of both signal joins (SJs) and coding joins (CJs) lead to inversion of the GFP cassette. Shown in this diagram is a schematic representation of unrearranged (UR) cleavage intermediates (second line), and four possible joining or partial joining products can be distinguished by Southern blotting (I–IV). I, both SJ and CJ fail to form. The GFP probe detects a 0.85-blunt 5′-phosphorylated RS ends (SE) and covalently sealed (hairpinned) coding ends (CE) fragment (red boxes in *A*–*C*) in EcoRV-digested DNA. A C4 probe detects the 2.2-kb 3′CE fragment in EcoRV-digested DNA. II, the SJ forms, but the CJ fails to form. The GFP probe detects a 0.3-SJ–5′CE fragment (*B* and *C*) in EcoRV-digested DNA. The C4 probe detects the 2.2-kb 3′CE fragment in EcoRV-digested DNA. III, normal rearrangement and formation of CJ. The C4 probe detects a 3-kb fragment in EcoRV+ NcoI digested DNA. IV, formation of hybrid join (HJ) and loss of the GFP fragment. The C4 probe detects a 4-kb band in EcoRV+NcoI-digested DNA and a 4-kb band in EcoRV-digested DNA. Summary of the results. The conversion from II to I is because of the loss of SJ formation (accumulation of SEs). In WT cells treated with both ATM and DNA-PKcs inhibitors, we observed the accumulation of the 0.85-kb SE-CE fragments, indicating SJ defects (*B*). Similarly, in ATM-deficient cells treated with DNA-PKcs inhibitor, we observed the accumulation of the 0.85-kb SE-CE fragments (*C*). These data indicate that DNA-PKcs and ATM have overlapping roles in SJ formation during inverted V(D)J recombination.

1. Bredemeyer AL, et al. (2006) ATM stabilizes DNA double-strand-break complexes during V(D)J recombination. *Nature* 442:466–470.